Korean J. Chem. Eng., **20**(5), 819-828 (2003)

Studies of Surface and Gas Reactions in a Catalytically Stabilized Combustor

Yong-Seog Seo†, Kwang-Sup Song and Sung-Kyu Kang

Korea Institute of Energy Research, 71-2 Jang-dong, Yusung-gu, Daejeon 305-343, Korea
(*Received 5 February 2003 • accepted 24 April 2003*)

Abstract−A numerical investigation of a catalytically stabilized thermal (CST) combustor was conducted for a multi-channel catalyst bed, and both the catalyst bed and thermal combustor were simultaneously modeled. The numerical model handled the coupling of the surface and gas reaction in the catalyst bed as well as the gas reaction in the thermal combustor. The behavior of the catalyst bed was investigated at a variety of operating conditions, and location of the flame in the CST combustor was investigated via an analysis of the distribution of CO concentration. Through parametric analyses of the flame position, it was possible to derive a criterion to determine whether the flame is present in the catalyst bed or the thermal combustor for a given inlet condition. The results showed that the maximum inlet temperature at which the flame is located in the thermal combustor increased with increasing inlet velocity.

Key words: Surface Reaction, Gas Reaction, Catalytically Stabilized Combustor, Numerical Simulation

INTRODUCTION

The application of catalytic combustion to gas turbine combustors has been a subject of interest for the last two decades [Beebe et al., 2000; Kolaczkowski, 1995; Pfefferle and Pfefferle, 1987; Trimm, 1984]. Thermal NO_x represents the main pollutant produced by gas turbines using LNG as a fuel. The maximum temperature of the combustion gas entering the turbine blades of the gas turbine is based on the thermally allowable temperature of the turbine blades, which is about 900 °C for blades constructed of a super alloy metal or about 1,300 °C for ceramic turbine blades. The flame temperature in a conventional gas turbine combustor using flame combustion is typically above 1,500 °C, which leads to the generation of significant thermal NO_x emissions. However, if catalytic combustion is employed, the flame temperature can be easily controlled to temperatures below 1,500 °C. It is well known that, since catalytic combustion enables ultra lean combustion, NO_x emissions can be controlled to low levels, frequently in the single digits, i.e., less than 10 ppm [Beebe et al., 2000; Schlegel et al., 1996]. If the temperature of the combustion gas is reduced to below 1,500 °C by catalytic combustion, thermal NO_x emissions will be nearly at the zero level according to the Zel'dovich mechanism of thermal NO_x formation.

In order to develop a gas turbine combustor using catalytic combustion, several types of design concepts have been proposed. Sadamori [1999] reported on the development of a catalytic combustor in which the entire mixture of fuel and air is combusted within the catalyst bed. The temperatures in the catalyst bed increase to the adiabatic flame temperature of the mixture, about 1,300 °C; and new types of a high temperature catalyst, hexaaluminate, was used [Inoue et al., 1999; Jang et al., 1999]. This type of design requires a reliable high temperature catalyst even though its structure is relatively simple.

Furuya et al. [1995] developed an alternate type of catalytic combustor comprised of two parts: a catalyst bed and a thermal combustor. In this design, a fraction of the fuel and all of the air are fed to the catalyst bed, and the fractional feedstock is completely combusted over the catalyst bed. The remaining fuel is introduced separately into the thermal combustor, which is located downstream from the catalyst bed. An advantage of this design is that temperatures of the catalyst bed can be easily controlled at a low level, below 1,000 °C, by simply adjusting the fraction of fuel fed to the catalyst bed. This enables the use of commercial catalysts in the catalytic combustor of gas turbines. However, this design also has a weak point. Since the nozzle for feeding the fuel should be placed in the thermal combustor, non-uniform mixing of fuel and air may take place, which produces hot spots and high levels of thermal NO_x.

Another type of catalytic combustor for gas turbines is the catalytically stabilized thermal (CST) combustor where the entire mixture of fuel and air is fed to the catalyst bed. The fuel is partially combusted over the catalyst bed, and the partially burned mixture then flows to the thermal combustor, which is located downstream from the catalyst bed. In the case of the CST combustor, the catalyst bed plays a role in supporting flame combustion of the mixture in the thermal combustor. This design is considered to be the most reasonable system for use with commercial catalysts, and has been widely studied by numerous researchers [Beebe et al., 2000; Seo et al., 2000b; Dalla Betta and Nielsen, 1999].

Studies of the CST combustor have been conducted by both numerical and experimental investigations. In the numerical study, only one channel is typically selected to analyze the surface and gas reaction in the catalyst bed [Seo et al., 2000a; Mantzaras et al., 2000; Raja et al., 2000; Wanker et al., 2000; Kim et al., 1989]. However, since the catalyst bed is composed of a monolithic honeycomb with multi-channels, a numerical analysis using only a single channel cannot yield accurate, precise information on the CST combustor. Moreover, most studies have focused only on the catalyst bed, and the thermal combustor, which is located downstream from the catalyst bed, is excluded. In fact, the catalyst bed has a direct effect on the characteristics of the flame combustion in a thermal combustor. The catalyst bed is intimately associated with the thermal combustor. Thus it would be more profitable to simultaneously treat both the

†To whom correspondence should be addressed.
E-mail: ysseo@kier.re.kr

catalyst bed and the thermal combustor.

The goal of present study was to investigate a CST combustor numerically. To achieve this, a numerical simulation was carried out for a multi-channel catalyst bed, and models were simultaneously developed for both the catalyst bed and the thermal combustor. This would be expected to provide more practical information regarding the effects of the catalyst bed on flame combustion in a thermal combustor. The numerical simulation for the CST combustor is performed in an axisymmetric two-dimensional, steady state. The numerical model handles the coupling of the surface and gas reactions in the catalyst bed as well as gas reactions in the thermal combustor. The flows in each of the catalyst bed and the thermal combustor are treated as a laminar and turbulent flow, respectively. The governing equations are solved by using the FLUENT software [Fluent, 2002] and surface reactions on the catalytic surface are calculated by means of a user-defined function provided by the FLUENT program. In the case of the CST combustor, it is very important to control the operating parameters so that only surface reactions occur on the catalytic bed and the thermal combustor maintains flame combustion. For this purpose, the issue of whether gas reactions take place in the catalyst bed or the thermal combustor for a given operating condition was investigated.

MATHEMATICAL MODEL

The numerical simulation for the CST combustor was performed in an axisymmetric two-dimensional and steady state. The model handles the coupling of the surface and gas reactions in the catalyst bed, and the gas reactions in the thermal combustor. The flows in each of the catalyst beds and the thermal combustor are treated as laminar and turbulent flow, respectively. CH_4 and air were used as the fuel and oxidant, respectively. The governing equations of the mixture can be written as follows.

Continuity equation

$$\frac{\partial}{\partial x_i}(\rho u_i) = 0 \tag{1}$$

Momentum equation

$$\frac{\partial}{\partial x_j}(\rho u_i u_j) = -\frac{\partial p}{\partial x_i} + \frac{\partial \tau_{ij}}{\partial x_j} + \rho g_i \tag{2}$$

Energy equation

$$\frac{\partial}{\partial x_i}[\rho u_i(\rho E + p)] = -\frac{\partial}{\partial x_i}\left[k\frac{\partial T}{\partial x_i} + \sum_j h_j J_j + u_j(\tau_{ij})\right] + \sum_j h_j R_{g,j} \tag{3}$$

Species equation

$$\frac{\partial}{\partial x_i}(\rho u_i m_j) = -\frac{\partial}{\partial x_i} J_{j,i} + R_{g,j} \tag{4}$$

State equation

$$p = \rho RT \sum \frac{Y_i}{W_i} \tag{5}$$

In Eq. (3), the stress tensor τ_{ij} is given by

$$\tau_{ij} = \left[\mu\left(\frac{\partial u_i}{\partial x_j} + \frac{\partial u_j}{\partial x_i}\right)\right] - \frac{2}{3}\mu\frac{\partial u_l}{\partial x_l}\delta_{ij} \tag{6}$$

In Eqs. (3) and (4), the gas reaction rate for CH_4, $R_{g,j}$, is calculated for the following two-step reactions.

$$CH_4 + 1.5O_2 \rightarrow CO + 2H_2O \tag{7-1}$$

$$R_{CH_4} = A_{g,1}\exp\left(-\frac{E_{g,1}}{RT}\right)[C_{CH_4}]^{0.7}[C_{O_2}]^{0.8}$$

$$CO + 0.5O_2 \rightarrow CO_2 \tag{7-2}$$

$$R_{CO} = A_{g,2}\exp\left(-\frac{E_{g,2}}{RT}\right)[C_{CO}]^{1.0}[C_{O_2}]^{0.25}[C_{H_2O}]^{0.5}$$

where parameter values are:

$A_{g,1} = 5.012\times10^{11}$ kg·m$^{1.5}$/kmol$^{1.5}$·s
$A_{g,2} = 2.239\times10^{12}$ kg·m$^{2.25}$/kmol$^{1.75}$·s
$E_{g,1} = 2.0\times10^{8}$ J/kmol
$E_{g,2} = 1.7\times10^{8}$ J/kmol.

In Eq. (4), the diffusion flux $J_{i,j}$ is given by

$$J_{i,j} = -\rho D_{i,m}\frac{\partial m_i}{\partial x_j} \tag{8}$$

The boundary conditions are given as follows:
Inlet conditions:

$T = T_o$, $u_i = u_{i,o}$, $m_i = m_{i,o}$

where the subscript o refers to the initial value of each parameter.

Outlet conditions:

$$\frac{\partial T}{\partial x} = 0, \quad \frac{\partial u_i}{\partial x} = 0, \quad \frac{\partial m_i}{\partial x} = 0$$

Conditions at the catalytic surfaces in the catalyst bed:

$$J_i \cdot n = R_{w,i} \tag{9}$$

$$k\left(\frac{\partial T}{\partial x_i}\cdot n\right) + \sum_i h_i(J_i \cdot n) = \sum_i h_i R_{w,i} \tag{10}$$

Conditions at the wall of the thermal combustor and the outmost wall of the catalyst bed are set to an adiabatic condition.

The surface reaction of CH_4 can be written as the following one-step reaction [Eq. (11)]. The surface reaction rate for CH_4 over the catalytic surface deposited with a Pd catalyst is calculated by using Eq. (12), proposed by Hayes and Kolaczkowski [1997].

$$CH_4 + 2O_2 \rightarrow CO_2 + 2H_2O \tag{11}$$

$$R_w = \eta A_w \exp\left(-\frac{E_w}{RT}\right)[Y_{CH_4}]^{0.72} \tag{12}$$

where parameter values are:

$A_w = 2.84\times10^{5}$ kmol/m^2·s and
$E_w = 1.31\times10^{8}$ J/kmol.

The effectiveness factor in Eq. (12), η, addresses the diffusion effect of reactants in the catalyst, which can be calculated by Eqs. (13) and (14), as derived by Leung and Hayes [1996].

$$\eta = (1 + 0.87\phi^{1.33})^{-0.75} \tag{13}$$

$$\phi = \left(\frac{L_c k_s RT}{D_{eff} p Y_{ch4}^{0.28}}\right)^{0.5} \tag{14}$$

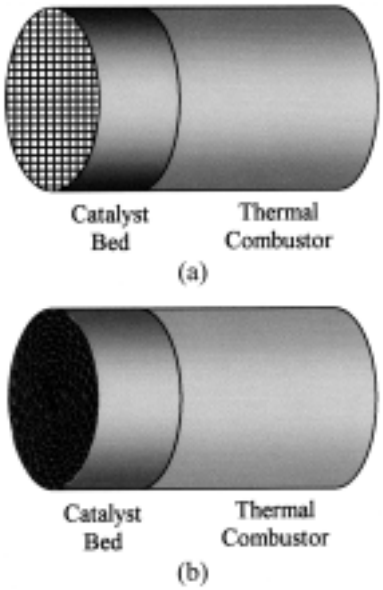

Fig. 1. Schematic of a CST combustor using (a) monolithic ceramic honeycomb and (b) corrugated metal honeycomb. The CST combustor is composed of a catalyst bed, placed upstream, and a thermal combustor, placed downstream.

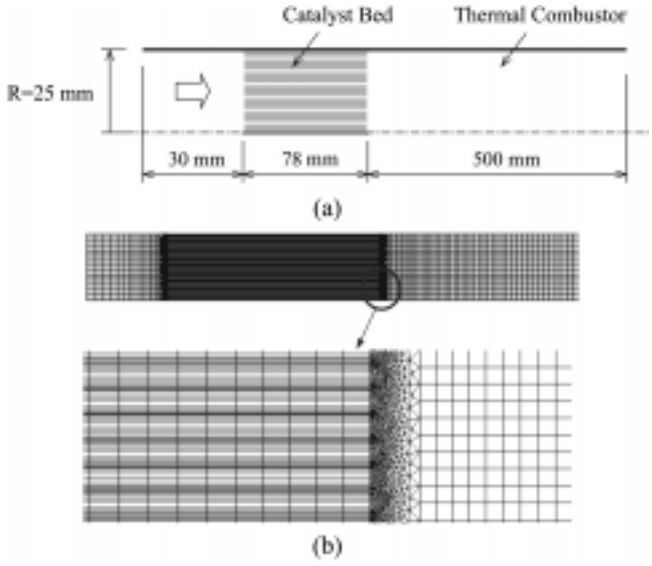

Fig. 2. (a) Computational domain for the numerical simulation of a CST combustor with an axisymmetric two-dimensional system and (b) its grid system.

where L_c is the thickness of the catalyst (=20.0×10^{-6} m), and

$$k_s = A_w \exp\left(-\frac{E_w}{RT}\right) \tag{15}$$

$$D_{eff} = 0.125\left(\frac{1}{D_{ab}} + \frac{1}{D_k}\right)^{-1} \tag{16}$$

In Eq. (15), A_w and E_w are the same as were used in Eq. (12). D_{ab} and D_k in Eq. (16) are the bulk diffusion coefficient (=$9.87\times10^{-10}T^{1.75}$) and the Knudsen diffusion coefficient (=$6.0625\times10^{-8}T^{0.5}$) in the catalyst, respectively.

Fig. 1 shows a schematic for the CST combustor, where (a) and (b) correspond to an example employing a monolithic ceramic honeycomb and a corrugated metal honeycomb, respectively, in the catalyst bed. The present numerical simulation simultaneously models both the catalyst bed and thermal combustor. This method is expected to provide more practical information on the effects of the catalyst bed on flame combustion in the thermal combustor. Most studies of CST combustors have been conducted by separately investigating the catalyst bed and the thermal combustor, which makes it difficult to collect accurate information regarding the coupling of the catalyst bed with the thermal combustor. Furthermore, the present study models the entire catalyst bed with multi channels as a computational domain. Studies to date typically treat only one channel for the catalyst bed, which makes the calculation relatively easy. However, the modeling of only one channel is unlikely to provide detailed information on the coupling of the surface reaction in the catalyst bed and the gas reaction in the thermal combustor.

Several types of catalysts can be used in a CST combustor. Typical examples are the monolithic ceramic honeycomb and the corrugated metallic honeycomb, as shown in Fig. 1. To model these types of catalysts, the catalyst bed is simplified as multi-layered catalyst surfaces (see Fig. 2). This simplification would be expected to make the calculation quite easy even though it is likely to provide a less accurate prediction in comparison with the practical catalyst. To model the catalyst bed without any simplification requires a computational memory of extremely large size, which makes a numerical calculation nearly impossible.

The computational domain and grid system for the CST combustor are shown in Fig. 2(a) and (b). The radius of the CST combustor is set to 25 mm, and the length of the catalyst bed and the thermal combustor is set to 78 mm and 500 mm, respectively. The gap between the catalytic surfaces in the catalyst bed is kept to 1.5 mm, which corresponds to a ceramic honeycomb having a cell size of 300 to 400 cells/inch. A grid system is composed of about 16,400 quadrilateral and triangular cells. The grids in the catalyst bed are made by using a non-uniform grading scheme so that the grids near catalytic surfaces are closer to one another. To solve the governing Eqs. (1)-(5), the FLUENT software [Fluent, 2002] is used and the surface reaction on catalytic surface is calculated by means of its user-defined functions.

Surface reactions are initiated only if the temperature of the catalytic surface reaches the ignition temperature of surface reaction. Thus, the mixture of air and fuel supplied to the catalyst bed must be heated to the ignition temperature of catalytic reaction by means of a pre-heating device. Once the surface reaction starts, the mixture flowing over the catalytic surface is heated by the heat generated from surface reactions. If the mixture is heated higher than the flame ignition temperature, a gas reaction is initiated. In this case, the gas reactions and surface reactions proceed simultaneously in the catalyst bed and the thermal combustor. For this reason, the catalyst bed is modeled by taking both surface and gas reaction into consideration, and the thermal combustor is modeled for a gas reaction.

RESULTS AND DISCUSSION

1. Behavior in the Catalyst Bed

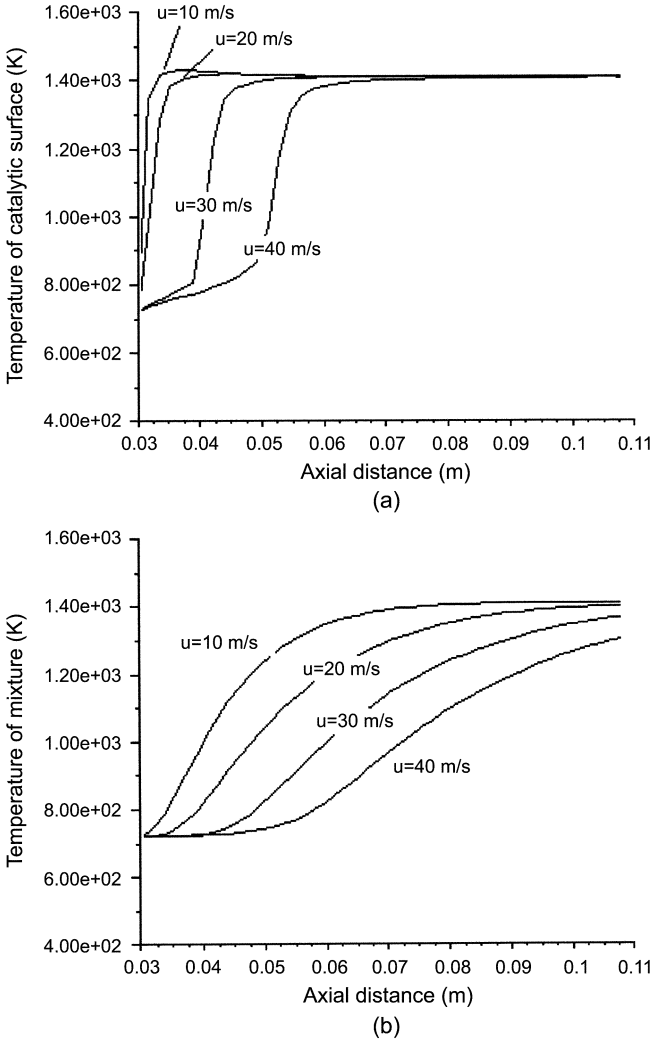

Fig. 3. Temperature profiles at each inlet velocity. For this calculation, the inlet temperature and methane/air volume ratio were set at 450 °C and 3.08%, respectively. (a) wall temperature at the catalytic surface and (b) mixture temperature at the channel center.

The catalyst bed, located in the fore part of the CST combustor, is considered to strongly affect the characteristics of the entire CST combustor, and the behavior in the catalyst bed was first investigated at a variety of operating conditions. Included among the operating conditions for the CST combustor are inlet temperature, inlet velocity and fuel concentration (fuel/air volume ratio).

The influence of inlet velocity on surface reaction in the catalyst bed was first investigated, and these data are plotted in Fig. 3. The higher inlet velocity shifts the ignition position of the surface reaction in a downstream direction. Here the ignition of surface reaction is defined as the state where the wall temperature begins to rise steeply, which can obviously be seen at an inlet velocity of 40 m/s in Fig. 3(a). In the case of a 10 m/s inlet velocity, the surface reaction begins when the mixture enters the catalyst bed, and the wall temperature rises to a maximum, the adiabatic temperature of the mixture. As the inlet velocity increases to 40 m/s, the catalytic ignition point moves about 0.02 m downstream in the catalyst bed. Fig. 3(b) shows the temperature of the mixture at different inlet velocities. As expected, the temperatures of the mixture are lower than the corresponding wall temperatures. This is because the surface reaction occurs first at the catalytic wall before the start of the gas reaction, and the heat generated from the surface reaction is transferred to the mixture flowing through the channels. At a sufficient distance in the channel, the wall and mixture temperatures then become the same, shown in case of 10 m/s inlet velocity.

Fig. 4 illustrates mass fraction profiles for methane, a feedstock, at the channel center. The mass fractions of methane drop exponentially along the axial distance at each inlet velocity. However, the rate of decrease in the mass fraction of methane is higher with less inlet velocity, which is in agreement with the trend of the wall temperature at the same inlet velocity. For surface reactions, the reactants diffuse into the catalytic surface, which induces a gradient for the reactants across the radial direction of the catalytic channel. Thus, examining mass fractions of methane at both the channel cen-

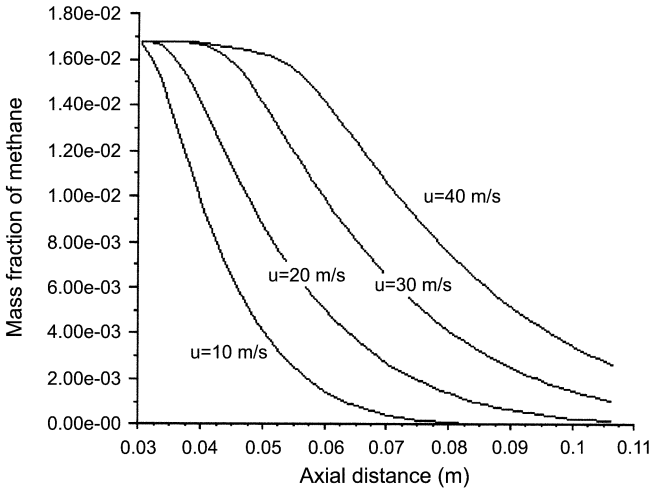

Fig. 4. Predicted mass fraction of methane at the channel center for various inlet velocities. Inlet conditions for the calculation were set at the same as those in Fig. 3.

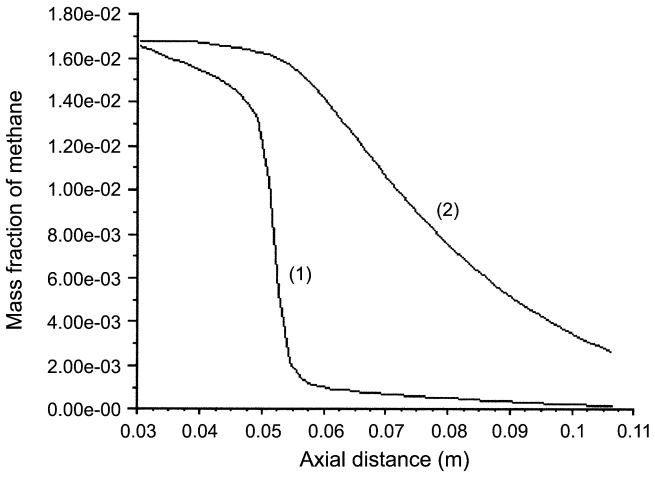

Fig. 5. Mass fraction profiles for methane at (1) the catalytic surface and (2) the channel center for the case of an inlet velocity of 40.0 m/s. Other inlet conditions for the calculation were set at the same as those in Fig. 3.

ter and the catalytic surface can provide in-depth information on the behavior of the catalytic reaction. Fig. 5 compares mass fraction profiles at each of the channel centers and the catalytic surface, and a considerable difference is evident. Near the inlet of the catalyst bed, the mass fraction at the catalytic surface, line (1) in Fig. 5, is gradually reduced along the axial distance. In the region from 0.05 mm to 0.057 mm distance, it drastically drops, and thereafter it decreases very slightly along the axial distance.

The mass fraction profile at the catalytic surface, line (1) in Fig. 5, can be divided into three zones. The first zone is the region from 0.03 to 0.05 m in axial distance, where the mass fraction of methane decreases gradually along the axial distance. This zone is where the surface reaction begins and methane molecules begin to be oxidized over the catalytic surface. The second zone includes the region from a distance of 0.05 to 0.057 m, where the mass fraction of methane drops steeply to the lowest level. The drastic decrease in the methane mass fraction indicates that the rate of methane oxidation at the catalytic surface sharply increases. In this zone, there exists the largest difference between mass fractions of methane at the channel center and the catalytic surface. The reason for this is that the reaction rate at the catalytic surface becomes higher than the diffusion rate of methane to the catalytic surface. Such a region is called a kinetically controlled region. The last zone appears at a distance of 0.057 m, where the mass fraction of methane is its lowest. In this zone, the rate of the surface reaction is maintained high even though the diffusion rate barely increases. As a result, the large difference between the surface reaction rate and the diffusion rate of methane is maintained, resulting in the large difference between mass fractions of methane at the channel center and the catalytic surface. Such a region is called a diffusion- controlled region.

In the next step, the effect of inlet temperature on the surface reaction in the catalyst bed was investigated, Fig. 6. The inlet temperature, that is, the preheating temperature of the mixture, is a crucial parameter in terms of initiating and maintaining the surface reaction over catalysts. For a given inlet condition, 30.0 m/s of inlet velocity and a 3.08% fuel/air ratio, the surface reaction appears to be-

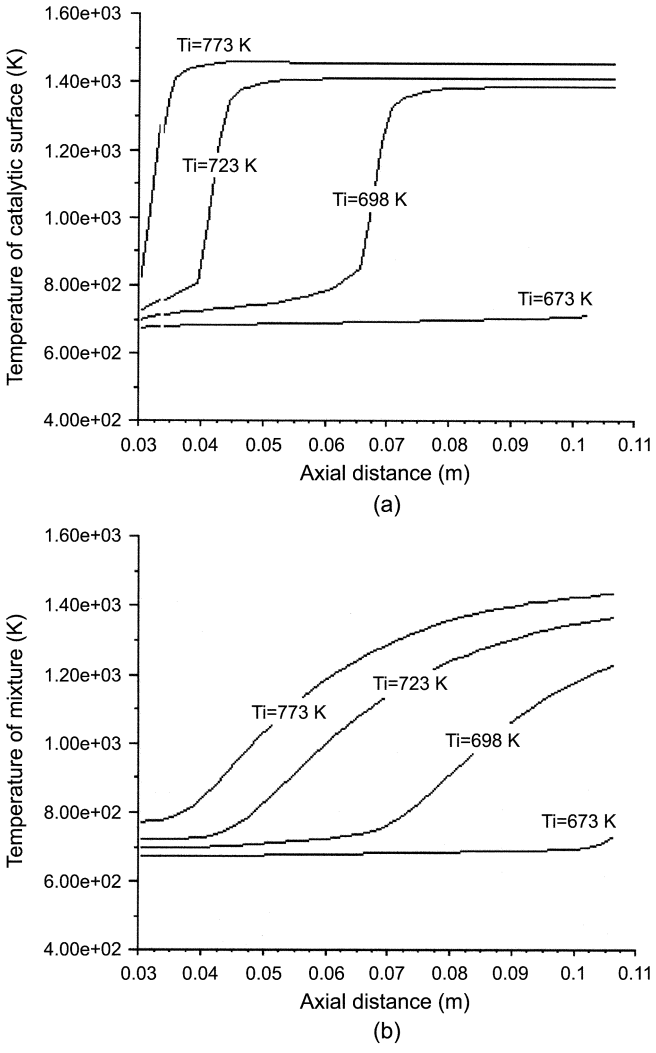

Fig. 6. Temperature profiles at each inlet temperature. For this calculation, the inlet velocity and methane/air volume ratio were set at 30.0 m/s and 3.08%, respectively. (a) wall temperature at the catalytic surface and (b) mixture temperature at the channel center.

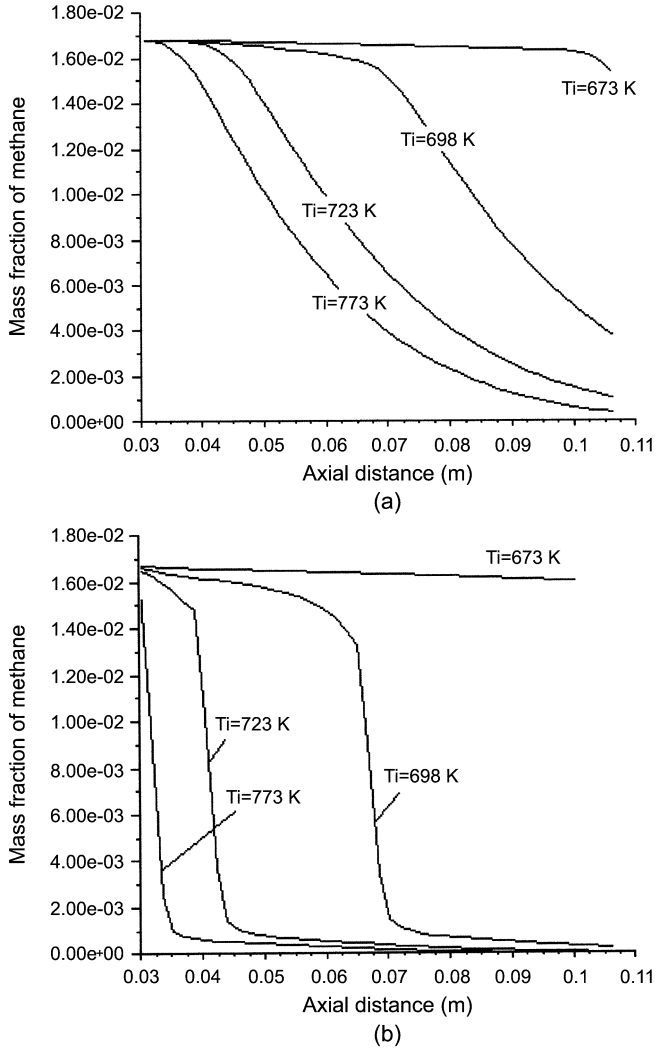

Fig. 7. Predicted mass fraction of methane at (a) the channel center and (b) the catalytic surface for various inlet temperatures. Inlet conditions for the calculation were set at the same as those in Fig. 6.

gin at an inlet temperature of more than 673 K. Once the surface reaction starts, the higher inlet temperature moves the position of the surface reaction in an upstream direction on the catalyst bed. For example, in the case of a high inlet temperature of 773 K, the surface reaction starts near the inlet of the catalyst bed. When designing a CST combustor, the selection of the appropriate inlet temperature which keeps the surface reaction stable in the catalyst bed for other given operating conditions is very important. The lowest inlet temperature should be selected on the basis of the ignition temperature of the surface reaction, while the highest inlet temperature is limited by the thermal stability of the catalysts.

Fig. 6(b) represents temperature profiles of mixtures at the channel center, which are lower than those at the catalytic wall, Fig. 6(a). This is because the surface reaction first takes place at the catalytic surface and the generated heat is then transferred to the mixture over the catalytic surface. The mass fractions of methane at channel center are also calculated with regard to inlet temperature at the same conditions as those shown in Fig. 6, and these results are shown in Fig. 7. Like Fig. 6, the position where the surface reaction begins to move upstream of the catalyst bed as the inlet temperature rises, and the mass fraction of methane drops exponentially along the axial distance.

Another important operating parameter is the fuel concentration, which determines the adiabatic combustion temperature of a mixture and also affects the surface reaction in the catalyst bed. The fuel concentration in the CST combustor was selected according to the maximum temperature required in a device to utilize the hot combustion gas. A typical example of the use of a CST combustor is a gas turbine, which normally requires a turbine inlet temperature of 900 to 1,300 °C. According to this requirement, the present study selected the range of 2.0 to 4.0% in methane/air volume ratio, which corresponds to an adiabatic combustion temperature of about 1,200 to 1,600 K. Fig. 8 illustrates the temperature profiles at the catalytic surface and the channel center for various fuel/air (F/A) ratios. As the fuel/air ratio increases, the ignition of a surface reaction takes place further upstream of the catalyst bed and the maximum temperature increases. The surface reaction rate for methane is proportional to the methane concentration [see Eq. (12)], so the higher fuel/air ratio generates a larger amount of heat, thereby the ignition point of catalytic reaction is maintained more upstream of the catalyst bed. Meanwhile, Fig. 9 denotes the mass fractions of

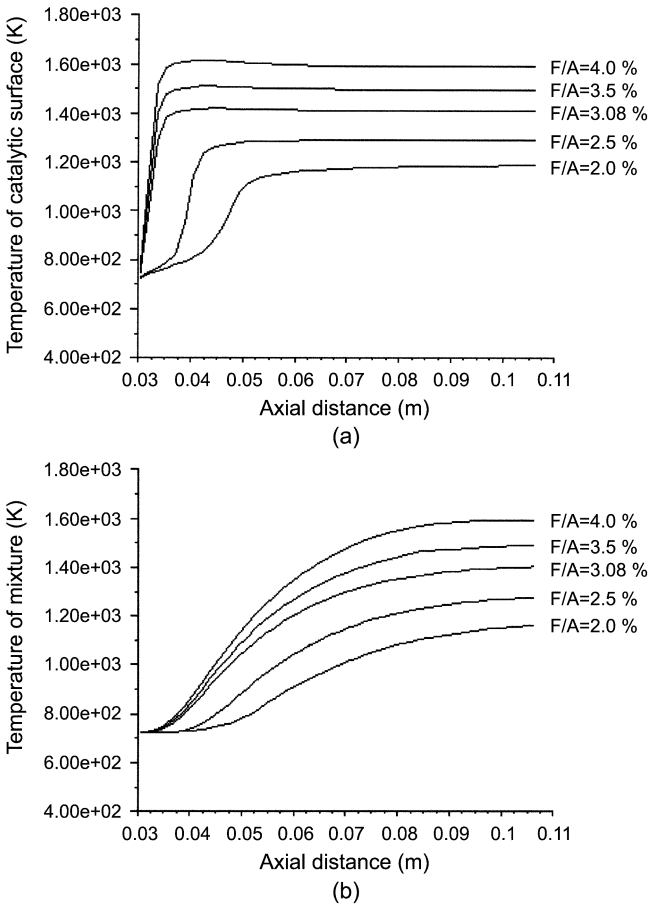

Fig. 8. Temperature profiles at each fuel/air ratio. For this calculation, the inlet velocity and inlet temperature were set at 20.0 m/s and 450 °C, respectively. (a) wall temperature at the catalytic surface and (b) mixture temperature at the channel center.

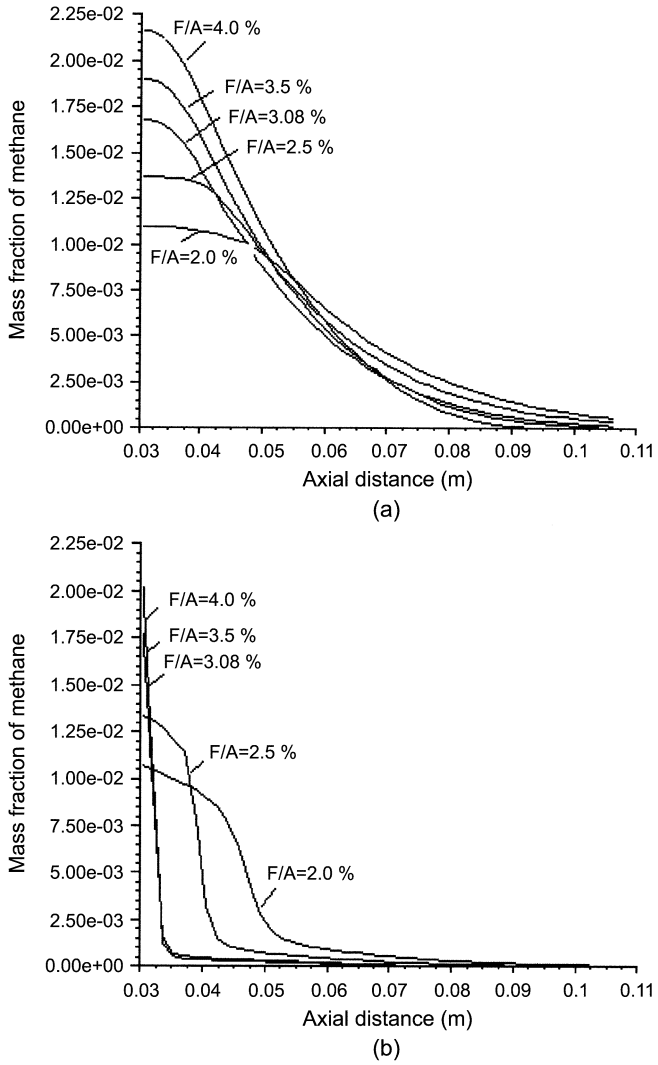

Fig. 9. Predicted mass fraction of methane at (a) the channel center and (b) the catalytic surface for various inlet temperatures. Inlet conditions for this calculation were set at the same as those in Fig. 8.

methane for various fuel/air ratios. Upstream of the catalyst bed, the higher fuel/air ratio shows a higher mass fraction of methane, but downstream, the situation is reversed, that is, the higher fuel/air ratio contains a lower mass fraction of methane [see Fig. 9(a)]. Especially, the cases of a fuel/air ratio of more than 3.08% encounter the kinetically controlled region just near the inlet of the catalyst bed [see Fig. 9(b)]. However, as the fuel/air ratio decreases, the kinetic control region moves toward the downward area of the catalyst bed.

Here it may be interesting to check the lean limit of the mixture of methane and air. In the case of flame combustion, the lean limit for a methane mixture is normally about 5.35% in fuel/air ratio at atmospheric conditions [Lewis and Elbe, 1961]. The present investigation, however, shows that catalytic combustion can burn stably with much leaner mixture in comparison with flame combustion. Fig. 8 shows that even at a low concentration, such as a fuel/air ratio of 2.0%, catalytic combustion takes place stably. Thus, catalytic combustion can be effectively used in combusting very lean mixtures and the combustion temperature can also be controlled by adjusting the fuel concentration entering the combustor.

2. Behavior in the Thermal Combustor

To stably combust a lean mixture in a CST combustor, the catalyst bed should support flame combustion in the thermal combustor via surface reactions. In a favorable system of the CST combustor, the catalyst bed is required to have only a surface reaction so that the catalytic wall temperature can be maintained within the thermally durable temperature range for the catalysts. The thermal combustor is required to burn fully the partially burned mixture flown out of the catalyst bed. Thus, to design a CST combustor, it is very important to predict whether the flame exists in the catalyst bed or the thermal combustor for a given operating conditions. Using a prediction for the presence of flame in the CST combustor, it is possible to design a CST combustor such that the flame is only in the thermal combustor, so that the catalyst bed keeps only a surface reaction without a flame. The location of the flame can be obtained via an analysis of CO concentration distribution, because the CO concentration in premixed combustion always rises sharply in the flame front. Thus, the present study also regards the peak position of CO concentration to be a flame position.

First, the temperature distribution in both the catalyst bed and the thermal combustor is plotted qualitatively in Fig. 10. In the analysis, the inlet temperature is changed stepwise from 400 °C to 500 °C, while other operating conditions are fixed to 20.0 m/s in inlet velocity and 3.08% in fuel/air ratio. At an inlet temperature of 400 °C, Fig. 10 (a), only the rear part of the catalyst bed shows a high temperature of more than 1,000 K, whereas the entire thermal combustor has a high temperature in excess of 1,000 K. This temperature distribution implies that the flame exists mainly in the thermal combustor, which can be checked, along with the CO distribution, later. As the inlet temperature increases to 450 °C, Fig. 10(b), a high temperature prevails in almost all the catalyst bed. In this case, the flame seems to be located within the catalyst bed, which can also be checked, along with CO analysis, later. When the inlet temperature rises further to 500 °C, the temperature distribution looks the same as that for a 450 °C inlet temperature except for the higher maximum temperature.

Fig. 11 describes CO distributions in both the catalyst bed and the thermal combustor at the same operating conditions as Fig. 10. At an inlet temperature of 400 °C, the peak for CO distribution is located in the rear part of the thermal combustor. The level of CO concentration in the catalyst bed appears to be nearly zero, which explains the existence of a flame in the thermal combustor. As the inlet temperature rises to 450 °C and 500 °C, the peak positions for CO concentration move within the catalyst bed. At these inlet temperatures, the flame is in the catalyst bed. Out of these two cases, the higher inlet temperature, 500 °C, shows that the peak position of CO concentration moves toward a more upstream location in the catalyst bed. These analyses demonstrate that the position where

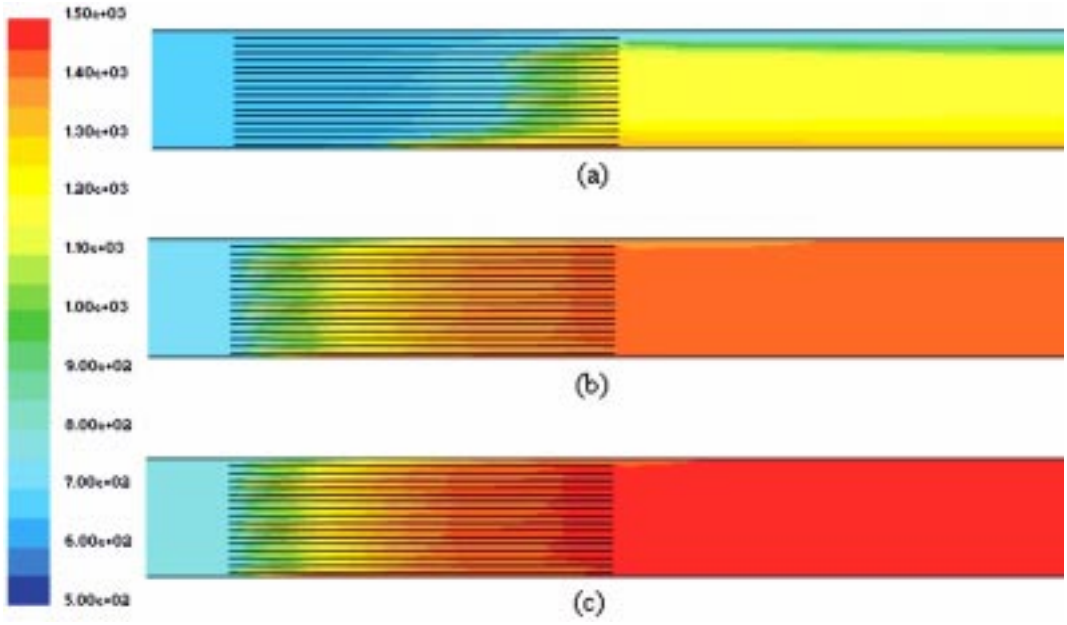

Fig. 10. Temperatures in the catalyst bed and thermal combustor at an inlet temperature of (a) 400 °C, (b) 450 °C and (c) 500 °C. Other inlet conditions for this calculation were set at 20.0 m/s in inlet velocity and 3.08% in fuel/air ratio.

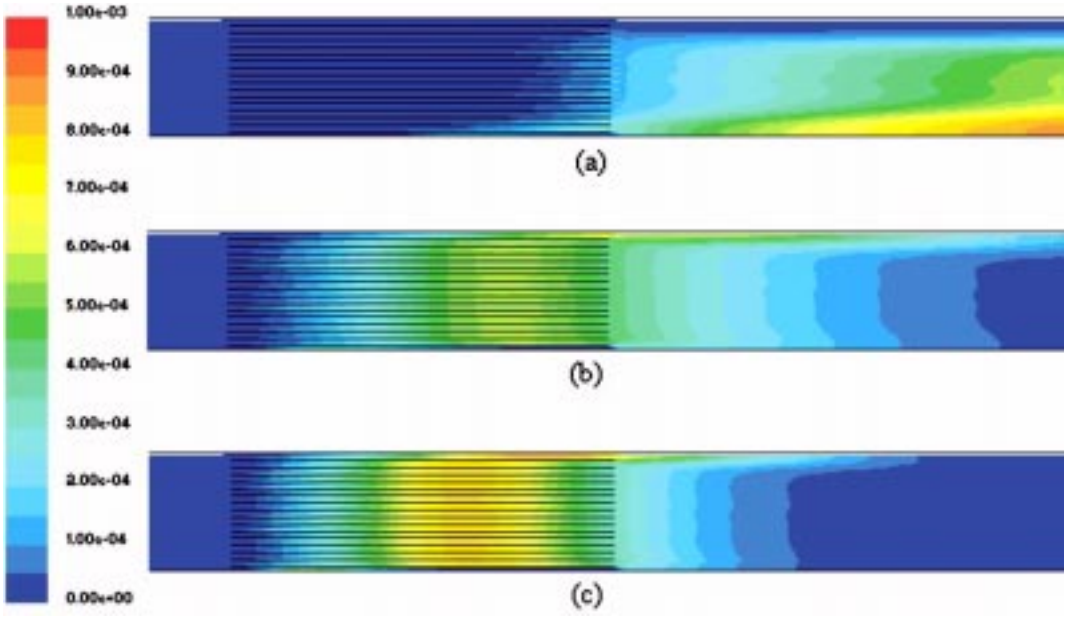

Fig. 11. CO distributions in the catalyst bed and thermal combustor at an inlet temperature of (a) 400 °C, (b) 450 °C and (c) 500 °C. Other inlet conditions for this calculation were set at the same as those of Fig. 10.

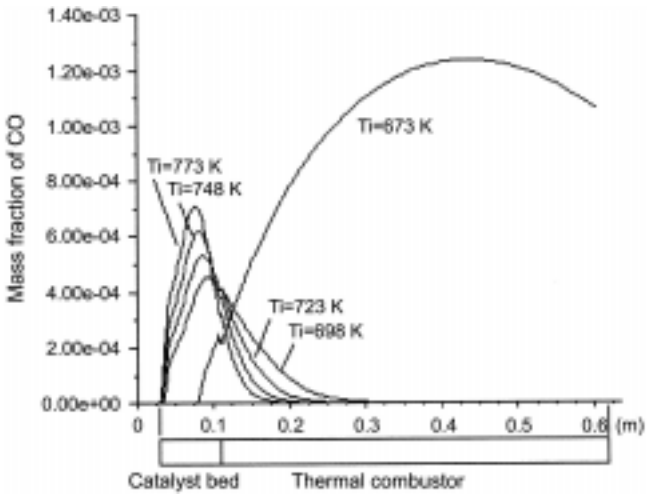

Fig. 12. CO profiles in the catalyst bed and thermal combustor for various inlet temperatures. Other inlet conditions for this calculation were set at the same as those in Fig. 10.

the flame exists can be determined through an analysis of CO distribution.

Meanwhile, Fig. 12 shows a quantitative profile for CO in the catalyst bed and the thermal combustor at the same operating conditions as Figs. 10 and 11. These data show that the inlet temperature significantly affects the CO concentration profile. As the inlet temperature rises, the peak position for the CO mass fraction moves from the thermal combustor to the catalyst bed. With a further increase in inlet temperature, the peak point within the catalyst bed shifts upstream. For the cases where the peak point for CO concentration is in the catalyst bed, the maximum value of CO concentration increases further with higher inlet temperatures. The reason for this is that the conversion rate of methane to CO is related directly to the temperature of the mixture [see Eq. (7-1)], which is related to the inlet temperature of the mixture. Moreover, the CO concentration drops to zero more quickly with increasing inlet temperature. Therefore, as long as the flame exists within the catalyst bed, the level of CO emission from the CST combustor would be expected to decrease with higher inlet temperature.

When the inlet temperature decreases further to 400 °C, the peak point of CO concentration moves to the thermal combustor from the catalyst bed. In this case, the flame exists in the thermal combustor of the CST combustor. When this CO profile is compared with the temperature distribution in Fig. 10(a), it is clear that the flame is located in the thermal combustor. An interesting issue here is that if the flame is in the thermal combustor, the maximum level of CO concentration increases more rapidly than the case where the flame is present in the catalyst bed. If we attempt to reduce CO emissions in the CST combustor, it is preferable to maintain the gas reaction in the catalyst bed. However, this requirement is difficult to achieve in practice because of the thermal durability of commercially available catalysts which force the flame to be maintained in the thermal combustor.

The effects of other inlet conditions on gas reactions are also investigated at a variety of operating conditions. Fig. 13 shows a plot of CO concentration at each inlet velocity. At a 450 °C inlet temperature and a 3.08% fuel/air ratio, the flame is located in the catalyst bed with an inlet velocity of less than 20 m/s. On the contrary, as the inlet velocity increases to more than 20 m/s, the flame is located in the thermal combustor. Like Fig. 12, the maximum value of CO concentration is much higher when flame is in the thermal combustor rather than in the catalyst bed.

Fig. 14 shows CO concentration profiles with regard to fuel concentration. This prediction demonstrates that the fuel/air ratio also has a significant effect on the flame position and the maximum value of CO concentration. When the fuel/air ratio is more than 3.08%, the flame is located in the catalyst bed. On the contrary, as the fuel/air ratio decreases to less than 3.08%, the flame exists in the ther-

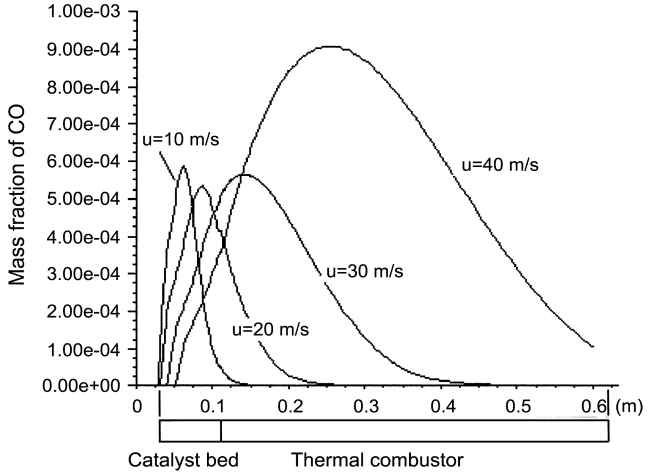

Fig. 13. CO profiles in the catalyst bed and thermal combustor for various inlet velocities. Other inlet conditions for this calculation were set at 450 °C in inlet temperature and 3.08% in fuel/air ratio.

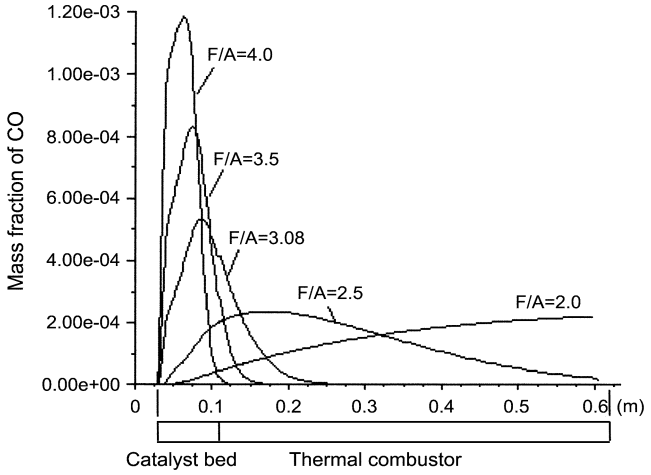

Fig. 14. CO profiles in the catalyst bed and thermal combustor for various fuel/air ratios. Other inlet conditions for this calculation were set at 20.0 m/s in inlet velocity and 450 °C in inlet temperature.

mal combustor. If the fuel/air ratio decreases to a very low value, 2.0%, the combustion appears to be incomplete within a selected length of the thermal combustor, 0.6 m. For this case, it becomes necessary to lengthen the thermal combustor or to employ additional devices to stabilize the flame.

When integrating the information obtained through the above analyses, it is possible to derive a criterion for deciding whether the flame exists in the catalyst bed or the thermal combustor for a given inlet condition. Fig. 15 is a graph explaining the flame location in the CST combustor. In the figure, Zones I and II correspond to operating conditions in which the flame exits in the catalyst bed and the thermal combustor, respectively. As an example, when an inlet velocity of 20.0 m/s is selected, the inlet temperature of the mixture, i.e., preheating temperature, should be less than 673 K if the flame is maintained only in the thermal combustor. The maximum inlet temperature at which the flame is located in the thermal combustor increases with inlet velocity. This criterion regarding flame location, obtained on the basis of the peak position of CO concentration, can be very useful in designing a CST combustor.

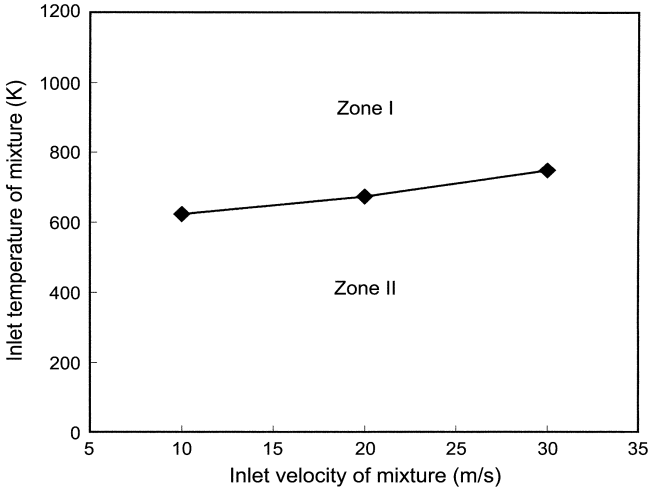

Fig. 15. Flame location in the CST combustor as a function of inlet conditions. Zones I and II correspond to operating conditions at which flame exists in the catalyst bed and the thermal combustor, respectively. The fuel/air ratio for this calculation was fixed at 3.08%.

CONCLUSIONS

Numerical investigation of a CST combustor was conducted with a multi-channel catalyst bed and was also modeled simultaneously for both the catalyst bed and thermal combustor. The numerical simulation was performed in an axisymmetric two-dimensional and steady state. The numerical model handled the coupling of surface and gas reactions in the catalyst bed, and the gas reaction in the thermal combustor. The flow in each of the catalyst bed and the thermal combustor was treated as a laminar and turbulent flow, respectively.

Behaviors in the catalyst bed were first investigated at a variety of operating conditions. An analysis of inlet velocity shows that a higher inlet velocity shifts the ignition position for surface reaction toward the downstream direction of the catalyst bed. A comparison between mass fraction profiles at each channel center and catalytic surface shows that three distinct zones exist along the axial distance: surface reaction ignition region, kinetically controlled region, and diffusion-controlled region. Meanwhile, as the fuel/air ratio increases, the ignition of surface reaction takes place more upstream of the catalyst bed and the maximum temperature increases. In the case of flame combustion, the lean limit for the methane mixture is normally about 5.35% in fuel/air ratio at atmospheric conditions. The present investigation, however, shows that catalytic combustion can burn stably at much more lean mixtures, even at a 2.0% fuel/air ratio.

As a favorable system of the CST combustor, a catalyst bed is required to have only a surface reaction so that the catalytic wall temperature can be maintained within the thermally durable temperature for the catalysts used. The thermal combustor is also required to fully combust the partially burned mixture flowing out of

the catalyst bed. For this purpose, the location of the flame was investigated through an analysis of the distribution of CO concentration. The results show that the inlet temperature has a significant effect on the CO concentration profile. As the inlet temperature rises, the peak position of CO mass fraction moves from the thermal combustor to the catalyst bed. For cases where the peak point of CO concentration is in the catalyst bed, the maximum value of CO concentration increases with higher inlet temperatures. It was also possible to derive a criterion for deciding whether the flame exists in the catalyst bed or the thermal combustor for a given inlet condition. This criterion could be very useful in designing a CST combustor. The maximum inlet temperature at which the flame is located in the thermal combustor increases with inlet velocity.

ACKNOWLEDGMENTS

The authors acknowledge the financial support from the Korean Ministry of Science and Technology through the NRL (National Research Laboratory) program.

NOMENCLATURE

A_g : pre-exponential factor in Eq. (7), related with reaction order
A_w : pre-exponential factor in Eq. (12) [kmol/m^{2}s]
C : molar concentration [kmol/m^3]
D_i : diffusion coefficient of species i [m^2/s]
$D_{i,m}$: diffusion coefficient of species i in the mixture [m^2/s]
D_{ab} : bulk diffusion coefficient [m^2/s]
D_{eff} : effective diffusion coefficient [m^2/s]
D_k : Knudsen diffusion coefficient [m^2/s]
E : internal energy [J/kg]
E_g : activation energy in Eq. (7) [J/kmol]
E_w : activation energy in Eq. (12) [J/kmol]
g : gravitational force [m/s^2]
h : enthalpy [J/kg]
$J_{i,j}$: diffusion flux of species i [kg/m^{2}s]
k : thermal conductivity [W/mK]
k_s : rate constant based on catalyst surface area [kg/m^{2}s]
L_c : thickness of washcoat [m]
m_i : mass fraction of species i
n : unit vector normal to catalyst surface
p : pressure [Pas]
R : universal gas constant [8.314 J/molK]
R_g : gas reaction rate [kg/m^{3}s]
R_w : surface reaction rate [kg/m^{2}s]
T : temperature [K]
u_i : i-directional velocity [m/s]
W_i : molecular weight of species i [kg/kmol]
Y_i : mole fraction of species i

Greek Letters

ϕ : Thiele modulus
η : effectiveness factor
μ : viscosity [Pas]
ρ : density [kg/m^3]
τ : stress tensor
δ_{ij} : Kronecker symbol

REFERENCES

Beebe, K. W., Cairns, K. D., Pareek, V. K., Nickolas, S. G., Schlatter, J. C. and Tsuchiya, T., "Development of Catalytic Combustion Technology for Single-digit Emissions from Industrial Gas Turbines," *Catalysis Today*, **59**, 95 (2000).

Dalla Betta, R. A. and Nielsen, T. R., "Application of Catalytic Combustion to a 1.5 MW Industrial Gas Turbine," *Catalysis Today*, **47**, 369 (1999).

Fluent software, "FLUENT User's Guide," Fluent Incorporated, http://www. fluent.com (2002).

Furuya, T., Sasaki, K., Hanakata, Y., Ohhashi, T., Yamada, M., Tsuchiya, T. and Furuse, Y., "Development of a Hybrid Catalytic Combustor for a 1,300 °C Class Gas Turbine," *Catalysis Today*, **26**, 345 (1995).

Hayes, R. E. and Kolaczkowski, S. T., "Introduction to Catalytic Combustion," Gordon and Breach Science Publishers, 169 (1997).

Inoue, H., Sekizawa, K., Eguchi, K. and Arai, H., "Thick-Film Coating of Hexaaluminate Catalyst on Ceramic Substrates for High-temperature Combustion," *Catalysis Today*, **47**, 181 (1999).

Jang, B. W., Nelson, R. M., Spivey, J., Ocal, M., Oukaci, R. and Marcelin, G., "Catalytic Oxidation of Methane over Hexaaluminates and Hexaaluminate-supported Pd Catalysts," *Catalysis Today*, **47**, 103 (1999).

Kim, D. K., Lee, S. B. and Yoon, P., "Numerical Simulation of Fixed-bed Catalytic Reactor for Isopropyl Alcohol Synthesis," *Korean J. Chem. Eng.*, **6**(2), 99 (1989).

Kolaczkowski, S. T., "Catalytic Stationary Gas Turbine Combustor: A Review of the Challenges Faced to Clear the Nest Set of Hurdles," *Trans IchemE.*, **73**, Part A, 168 (1995).

Leung, D. and Hayes, R. E., "Diffusion Limitation Effects in the Washcoat of a Catalytic Monolith Reactor," *The Canadian Journal of Chemical Engineering*, **74**, 94 (1996).

Lewis, B. and Guenther von Elbe, "Combustion Flames and Explosions of Gases," Academic Press (1961).

Mantzaras, J., Appel, C., Benz, P. and Dogwiler, U., "Numerical Modeling of Turbulent Catalytically Stabilized Channel Flow Combustion," *Catalysis Today*, **59**, 3 (2000).

Pfefferle, L. D. and Pfefferle, W. C., "Catalysis in Combustion," *Catal. Rev.-Sci. Eng.*, **29**(2&3), 219 (1987).

Raja, L. L., Kee, R. J., Deutschmann, O., Warnatz, J. and Schmidt, L. D., "A Critical Evaluation of Navier-Stokes, Boundary-layer and Plug-flow Models of the Flow and Chemistry in a Catalytic-combustion Monolith," *Catalysis Today*, **50**, 47 (2000).

Sadamori, H., "Application Concepts and Evaluation of Small-scale Catalytic Combustors for Natural Gas," *Catalysis Today*, **47**, 325 (1999).

Seo, Y. S., Cho, S. J., Kang, S. K. and Shin, H. D., "Numerical Studies of Catalytic Combustion in a Catalytically Stabilized Combustor," *International Journal of Energy Research*, **24**, 1049 (2000a).

Seo, Y. S., Cho, S. J., Kang, S. K. and Shin, H. D., "Experimental and Numerical Studies on Combustion Characteristics of a Catalytically Stabilized Combustor," *Catalysis Today*, **59**, 75 (2000b).

Trimm, D. L., "Catalytic Combustion (Review)," *Appl. Catal.*, **7**, 249 (1984).

Wanker, R., Raupenrauch, H. and Staudinger, G., "A Fully Distributed Model for the Simulation of a Catalytic Combustor," *Chemical Engineering Science*, **55**, 4709 (2000).